6

DFT Based Channel Estimation Methods for MIMO-OFDM Systems

Moussa Diallo[1], Maryline Hélard[2], Laurent Cariou[3] and Rodrigue Rabineau[4]
[1,3,4]*Orange Labs, 4 rue du Clos Courtel, 35512 Cesson-Sévigné Cedex*
[2]*INSA IETR, UEB, 20 Avenue des Buttes de Coesmes, CS 70839, 35708 Rennes Cedex 7*
France

1. Introduction

The great increase in the demand for high-speed data services requires the rapid growth of mobile communications capacity. Orthogonal frequency division multiplexing (OFDM) provides high spectral efficiency, robustness to intersymbol interference (ISI), as well as feasibility of low cost transceivers (Weinstein & Ebert, 1971). Multiple input multiple output (MIMO) systems offer the potential to obtain a diversity gain and to improve system capacity (Telatar, 1995), (Alamouti, 1998), (Tarokh et al., 1999). Hence the combination of MIMO and OFDM techniques (MIMO-OFDM) is logically widely considered in the new generation of standards for wireless transmission (Boubaker et al., 2001). In these MIMO-OFDM systems, considering coherent reception, the channel state information (CSI) is required for recovering transmitted data and thus channel estimation becomes necessary.
Channel estimation methods can be classified into three distinct categories: blind channel estimation, semi-blind channel estimation and pilot-aided channel estimation. In the pilot-aided methods, pilot symbols known from the receiver are transmitted as a preamble at the beginning of the frame or scattered throughout each frame in a regular manner. On the contrary, in blind methods, no pilot symbols are inserted and the CSI is obtained by relying on the received signal statistics (Winters, 1987). Semi-blind methods combine both the training and blind criteria (Foschini, 1996). In this paper, we focus our analysis on the time domain (TD) channel estimation technique using known reference signals. This technique is attractive owing to its capacity to reduce the noise component on the estimated channel coefficients (Zhao & Huang, 1997).
The vast majority of modern multicarrier systems contain null subcarriers at the spectrum extremities in order to ensure isolation from/to signals in neighboring frequency bands (Morelli & Mengali, 2001) as well as to respect the sampling theorem (3GPP, 2008). It was shown that, in the presence of these null subcarriers, the TD channel estimation methods suffer from the "border effect" phenomenon that leads to a degradation in their performance (Morelli & Mengali, 2001). A TD approach based on pseudo inverse computation is proposed in (Doukopoulos & Legouable, 2007) in order to mitigate this "border effect". However the degradation of the channel estimation accuracy persists when the number of the null subcarriers is large.
In this document, we look at various time domain channel estimation methods with this constraint of null carriers at spectrum borders. We show in detail how to gauge the importance

of the "border effect" depending on the number of null carriers, which may vary from one system to another. Thereby we assess the limit of the technique discussed in (Doukopoulos & Legouable, 2007) when the number of null carriers is large. Finally the DFT with the truncated singular value decomposition (SVD) technique is proposed to completely eliminate the impact of the null subcarriers whatever their number. A technique for the determination of the truncation threshold for any MIMO-OFDM system is also proposed.
The paper is organized as follows. Section 2 describes the studied MIMO-OFDM system, including the construction of the training sequences in the frequency domain and the least square (LS) channel estimation component. Then section 3.1 presents the main objectives (*noise reduction* and *interpolation*) of the classical DFT based channel estimation and its weakness regarding the "border effect". The pseudo inverse concept is then studied in section 4. Next, the DFT with truncated SVD is detailed in section 5. Finally, the efficiency of these channel estimators is demonstrated in section 6 for two distinct application environments: *indoor* and *outdoor* respectively applying 802.11n and 3GPP system parameters.
Notations: Superscript † stands for pseudo-inversion. Operator e represents an exponential function. $(.^{H})$ stands for conjugation and transpose. C denotes a complex number set and $j^2 = -1$. $\| \|$ denotes the Euclidean norm.

2. MIMO-OFDM system model

The studied MIMO-OFDM system is composed of N_t transmit and N_r receiving antennas. Training sequences are inserted in the frequency domain before OFDM modulation which is carried out for each antenna.
The OFDM signal transmitted from the i-th antenna after performing IFFT (OFDM modulation) on the frequency domain signal $X_i \in C^{N\times 1}$ at time index n can be given by:

$$x_i(n) = \sqrt{\frac{1}{N}} \sum_{k=0}^{N-1} X_i(k) e^{j\frac{2\pi kn}{N}}, \qquad 0 \leq (n,k) \leq N \tag{1}$$

where N is the number of IFFT points and k the subcarrier index.
The baseband time domain channel response between the transmitting antenna i and the receiving antenna j under the multipath fading environments can be expressed as (Van de Beek et al., 1995):

$$h_{ij}(n) = \sum_{l=0}^{L_{ij}-1} h_{ij,l}\delta(n - \tau_{ij,l}) \tag{2}$$

with L_{ij} the number of paths, $h_{ij,l}$ and $\tau_{ij,l}$ the complex time varying channel coefficient and delay of the l-th path.
The use of the cyclic prefix (CP) allows both the preservation of the orthogonality between the tones and the elimination of the ISI between consecutive OFDM symbols.
At the receiver side, after removing the CP and performing the OFDM demodulation, the received frequency domain signal can be expressed as follows by using (1) and (2):

$$R_j(k) = \sum_{i=0}^{N_t-1} X_i(k) H_{ij}(k) + \Xi(k) \tag{3}$$

where $H_{ij}(k)$ is the discrete response of the channel on subcarrier k between the i-th transmit antenna and the j-th receiving antenna and Ξ_k the zero-mean complex Gaussian noise after the

FFT process. Then Least Square (LS) channel estimation is performed by using the extracted pilots.
In SISO-OFDM, without exploiting any knowledge of the propagation channel statistics, the LS estimates regarding the pilot subcarrier k can be obtained by dividing the demodulated pilot signal $R_j(k)$ by the known pilot symbol $X(k)$ in the frequency domain (Zhao & Huang, 1997). The LS estimates regarding the pilot subcarrier k can be expressed as follows:

$$H_{LS}(k) = H(k) + \Xi(k)/X(k). \tag{4}$$

Nevertheless in the MIMO-OFDM system, from (3), an orthogonality between pilots is mandatory to obtain LS estimates for each receiver antenna without interference from the other antennas. In this paper, we consider the case where the pilots from different transmit antennas are orthogonal to each other in the frequency domain. It is important to note that this orthogonality can also be obtained in the time domain by using the cyclic shift delay (CSD) method (Auer, 2004).
The orthogonality between pilots in the frequency domain can be obtained by different ways:

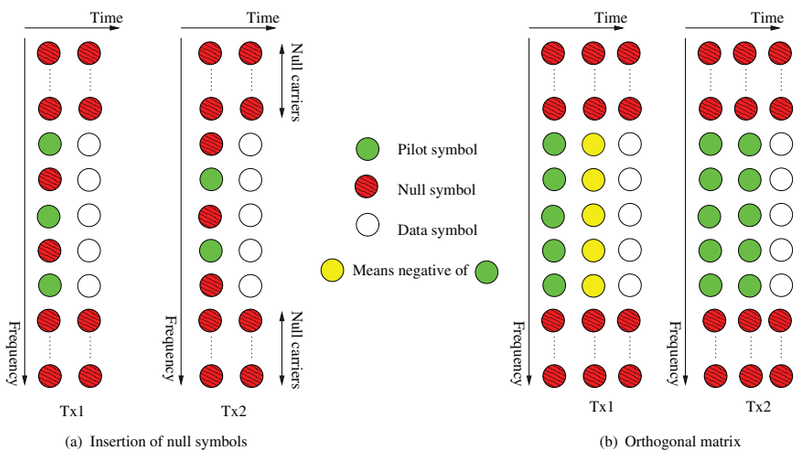

Fig. 1. Orthogonality between pilots in the frequency domain when $N_t = 2$.

- The orthogonality can be achieved with the use of transmission of pilot symbols on one antenna and of null symbols on the other antennas in the same instant (Fig. 1(a)). This solution is commonly and easily implemented in the presence of mobility as for instance in 3GPP/LTE (3GPP, 2008). Therefore LS estimates can only be calculated for M/N_t subcarriers, M representing the number of modulated subcarriers. Then interpolation must be performed in order to complete the estimation for all the subcarriers.
- The orthogonality can also be achieved using a specific transmit scheme represented by an orthogonal matrix. Fig. 1(b) represents the pilot insertion structure for a two transmit antenna system. The orthogonality between training sequences for antennas 1 and 2 is obtained by using the following orthogonal matrix.

$$\begin{bmatrix} 1 & -1 \\ 1 & 1 \end{bmatrix} \tag{5}$$

  This technique is frequently used when the channel can be assumed constant at least over the duration of N_t OFDM symbols in the case of quite slow variations. For instance, this

method is used in the wireless local area network (WLAN) IEEE802.11n system (802.11, 2007). LS estimates can be calculated for all the M modulated subcarriers with the use of full pilot OFDM symbols.

Assuming orthogonality between pilots, N_t LS estimation algorithms on pilot subcarriers can be applied per receive antenna:

$$H_{ij,LS}(k) = H_{ij}(k) + \Xi_{ij}(k)/X_{ij}(k). \tag{6}$$

Thus the LS estimation is computed for all the subchannels between the transmit and the receiver antennas. Nevertheless, it is important to note the two following points:

- From (6), it can be observed that the accuracy of LS estimated channel response is degraded by the noise component.
- To get an estimation for all the subcarriers, interpolation may be required depending on the pilots insertion scheme.

Time domain processing will then be used in order to improve the accuracy of the LS estimation of all the subchannels.

3. Classical DFT based channel estimation

In order to improve the LS channel estimation performance, the DFT-based method has been proposed first as it can advantageously target both noise reduction and interpolation purposes.

3.1 Main goals of DFT based channel estimation

3.1.1 Noise reduction

DFT-based channel estimation methods allow a reduction of the noise component owing to operations in the transform domain, and thus achieve higher estimation accuracy (Van de Beek et al., 1995) (Zhao & Huang, 1997). In fact, after removing the unused subcarriers, the LS estimates are first converted into the time domain by the IDFT (inverse discrete fourier transform) algorithm. A smoothing filter is then applied in the time domain assuming that the maximum multi-path delay is kept within the cyclic prefix (CP) of the OFDM symbol. As a consequence, the noise power is reduced in the time domain. The DFT is finally applied to return to the frequency domain. The smoothing process using DFT is illustrated in Fig.2.

3.1.2 Interpolation

DFT can be used simultaneously as an accurate interpolation method in the frequency domain when the orthogonality between training sequences is based on the transmission of scattered pilots (Zhao & Huang, 1997). The number ($N_p = M/N_t$) of pilot subcarriers, starting from the i-th subcarrier, is spaced every N_t subcarriers (Fig.1(a)). The LS estimates obtained for the pilot subcarriers given by (6) are first converted into the time domain by IDFT of length M/N_t. As the impulse response of the channel is concentrated on the CP first samples, it is possible to apply *zero-padding* (ZP) from M/N_t to $M-1$. The frequency channel response over the whole bandwidth is calculated by performing a M points DFT. It is obvious that N_t must satisfy the following condition:

$$N_t \leq \frac{M}{CP} \tag{7}$$

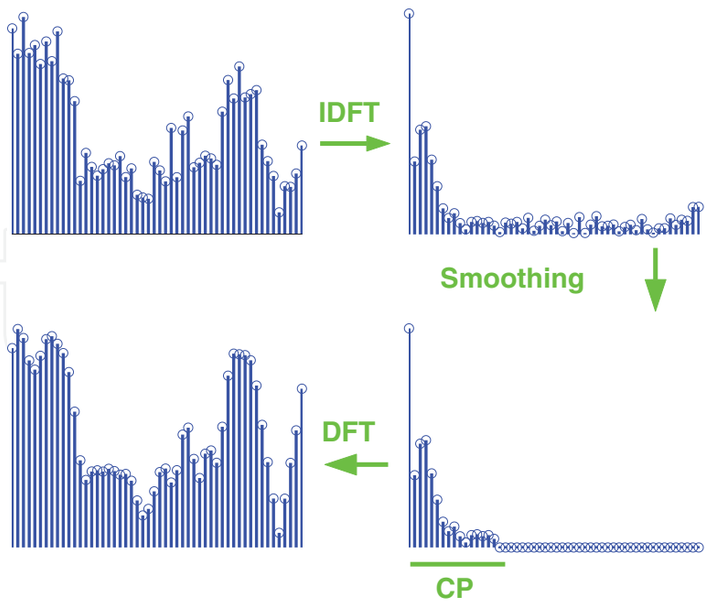

Fig. 2. Smoothing using DFT.

NB: In the rest of the paper, we will consider the case where $N_p = M$ for mathematical demonstrations in order to make reading easier. Otherwise if $N_p < M$ interpolation can be performed.

3.2 Drawback of DFT based channel estimation in realistic system

In a realistic context, only a subset of M subcarriers is modulated among the N due to the insertion of null subcarriers at the spectrum's extremities for RF mask requirements. The application of the smoothing filter in the time domain will lead to a loss of channel power when these non-modulated subcarriers are present at the border of the spectrum. That can be demonstrated by calculating the time domain channel response.
The time domain channel response of the LS estimated channel is given by (8). From (6) we can divide $h_{n,LS}^{IDFT}$ into two parts:

$$\begin{aligned} h_{ij,n,LS}^{IDFT} &= \sqrt{\frac{1}{N}} \sum_{k=\frac{N-M}{2}}^{\frac{N+M}{2}} H_{ij,k,LS} e^{j\frac{2\pi nk}{M}} \\ &= h_{ij,n}^{IDFT} + \xi_{ij,n}^{IDFT} \end{aligned} \tag{8}$$

where ξ_n^{IDFT} is the noise component in the time domain and h_n^{IDFT} is the IDFT of the LS estimated channel without noise. This last component can be further developed as follows:

$$\begin{aligned} h_{ij,n}^{IDFT} &= \sqrt{\frac{1}{N}} \sum_{k=N_b}^{N_e} \left(\sum_{l=0}^{L_{ij}-1} h_{ij,l} e^{-j\frac{2k\pi\tau_{ij,l}}{N}} \right) e^{-j\frac{2\pi kn}{N}} \\ &= \sqrt{\frac{1}{N}} \sum_{l=0}^{L_{ij}-1} h_{ij,l} \sum_{k=N_b}^{N_e} e^{-j\frac{2\pi k}{N}(\tau_{ij,l}-n)} \end{aligned} \tag{9}$$

where $N_b = (N-M)/2$ and $N_e = (N+M)/2 - 1$.
It can be seen from (9) that if all the subcarriers are modulated, i.e $M = N$, the last term of (9) $\sum_{k=\frac{N-M}{2}}^{\frac{N+M}{2}-1} e^{-j\frac{2\pi k}{N}(\tau_{ij,l}-n)}$ will verify:

$$\sum_{k=\frac{N-M}{2}}^{\frac{N+M}{2}-1} e^{-j\frac{2\pi k}{N}(\tau_{ij,l}-n)} = \begin{cases} N_p & n = \tau_{ij,l} \\ 0 & otherwise \end{cases} \tag{10}$$

where $\tau_{ij,l} = 0, 1, ..., L_{ij} - 1$ and $n = 0, ..., M - 1$.
From (10), we can safely conclude that:

$$h_{ij,n}^{IDFT} = 0 \; n = L_{ij}, ..., M \tag{11}$$

Assuming $CP > L_{ij}$, we do not lose part of the channel power in the time domain by applying the smoothing filter of length CP.
Nevertheless, when some subcarriers are not modulated at the spectrum borders, i.e. $M < N$, the last term of (9) can be expressed as:

$$\sum_{k=\frac{N-M}{2}}^{\frac{N+M}{2}-1} e^{-j\frac{2\pi k}{N}(\tau_{ij,l}-n)} = \begin{cases} M & n = \tau_{ij,l} \\ \frac{1-e^{-j2\pi\frac{M}{N}(\tau_{ij,l}-n)}}{1-e^{-j\frac{2\pi}{N}(\tau_{ij,l}-n)}} & n \neq \tau_{ij,l} \end{cases} \tag{12}$$

where $\tau_{ij,l} = 0, 1, ..., L_{ij} - 1$ and $n = 0, ..., M - 1$.
The channel impulse response $h_{ij,n}^{IDFT}$ can therefore be rewritten in the following form:

$$h_{ij,n}^{IDFT} = \frac{1}{\sqrt{N}} \begin{cases} M.h_{ij,l=n} + \sum_{l=0,l\neq n}^{L_{ij}-1} h_{ij,l} \frac{1-e^{-j2\pi\frac{M}{N}(\tau_{ij,l}-n)}}{1-e^{-j\frac{2\pi}{N}(\tau_{ij,l}-n)}}. & n < L_{ij} \\ \sum_{l=0}^{L_{ij}-1} h_{ij,l} \frac{1-e^{-j2\pi\frac{M}{N}(\tau_{ij,l}-n)}}{1-e^{-j\frac{2\pi}{N}(\tau_{ij,l}-n)}}. & L_{ij} - 1 < n < M \end{cases} \tag{13}$$

We can observe that $h_{ij,n}^{IDFT}$ is not null for all the values of n due to the phenomenon called here "Inter-Taps Interference (ITI)". Consequently, by using the smoothing filter of length CP in the time domain, the part of the channel power contained in samples $n = CP, ..., M - 1$ is lost. This loss of power leads to an important degradation on the estimation of the channel response. In OFDM systems, Morelli shows that when null carriers are inserted at the spectrum extremities, the performance of the DFT based channel estimation is degraded especially at the borders of the modulated subcarriers (Morelli & Mengali, 2001). This phenomenon is called the “border effect”. This “border effect” phenomenon is also observed in MIMO context (Le Saux et al., 2007).
In order to evaluate the DFT based channel estimation, the mean square error (MSE) performance for the different modulated subcarriers is considered in the following subsection.

3.3 MSE performance of DFT based channel estimation

In MIMO-OFDM context with N_t transmit antennas and N_r receive antennas, the (MSE) on the $k - th$ subcarrier is equal to:

$$MSE(k) = \frac{\sum_{i=0}^{N_t-1} \sum_{i=0}^{N_r-1} E\left[\left\|\widehat{H}(k) - H(k)\right\|^2\right]}{N_t N_r} \tag{14}$$

where $\widehat{H}(k)$ and $H(k)$ represent the estimated frequency channel response and the ideal one respectively.

MSE performance are provided here over frequency and time selective MIMO SCME (spatial channel model extension) channel model typical of macro urban propagation (Baum et al., 2005). The DFT based channel estimation is applied to a 2×2 MIMO system with the number of FFT points set equal to 1024. The orthogonality between pilots is obtained using null symbol insertion described in 2 and interpolation is performed to obtain channel estimates for all modulated subcarriers.

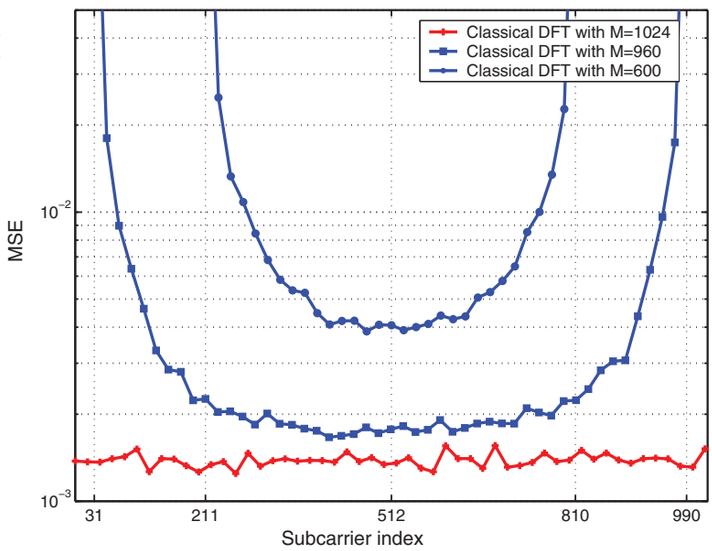

Fig. 3. Average mean square error versus subcarrier index for classical DFT based channel estimation. The number of modulated subcarrier are $M = 960$ and $M = 600$. $N_t = 2$, $N_r = 2$, $N = 1024$ and $SNR = 10dB$

Fig.3 shows the MSE performance of the different subcarriers when applying the classical DFT based channel estimation method depending on the number of modulated subcarriers. First, when all the subcarriers are modulated ($N = M = 1024$), there is no "border effect" and the MSE is almost the same for all the subcarriers. This is due to the fact that all the channel power is retrieved in the first CP samples of the impulse channel response (3.1). However when null subcarriers are inserted on the edge of the spectrum ($N \neq M$), the MSE performance is degraded by the loss of a part of the channel power in the time domain and then the "border effect" occurs. It is already noticeable that the impact of the "border effect" phenomenon increases greatly with the number of null subcarriers.
To mitigate this "'border effect" phenomenon, the pseudo inverse technique proposed in (Doukopoulos & Legouable, 2007) is studied in the next section.

4. DFT with pseudo inverse channel estimation

Classical DFT based channel estimation described in the previous section can be also expressed in a matrix form.

The unitary DFT matrix F of size $N \times N$ is defined with the following expression:

$$\mathrm{F} = \begin{bmatrix} 1 & 1 & 1 & \dots & 1 \\ 1 & W_N & W_N^2 & \dots & W_N^{N-1} \\ \vdots & \vdots & \vdots & \dots & \vdots \\ 1 & W_N^{N-1} & W_N^{2(N-1)} & \dots & W_N^{(N-1)(N-1)} \end{bmatrix} \tag{15}$$

where $W_N^i = e^{-j\frac{2\pi i}{N}}$.
To accommodate the non-modulated subcarriers, it is necessary to remove the rows of the matrix F corresponding to the position of those null subcarriers. Furthermore, in order to reduce the noise component in the time domain by applying smoothing filtering, only the first CP columns of F are used (Fig.2). Hence the *transfer matrix* becomes $F^{'} \in C^{M \times CP}$:
$F^{'} = F(\frac{N-M}{2} : \frac{N+M}{2} - 1, 1 : CP)$.
We can then express the impulse channel response, after the smoothing filter, in a matrix form:

$$h_{ij,LS}^{IDFT} = F^{'H} H_{ij,LS} \tag{16}$$

where $h_{ij,LS}^{IDFT} \in C^{CP \times 1}$, $H_{ij,LS} \in C^{M \times 1}$.
To reduce the "border effect" Doukopoulos propose the use of the following minimization problem (Doukopoulos & Legouable, 2007).

$$h_{ij,LS}^{pseudoinverse} = \arg\min_{h_{ij}} \left\| F' - H_{ij,LS} \right\|^2 \tag{17}$$

The idea that lies behind the above minimization problem is to reduce the "border effect", as illustrated in the figure 4, by minimizing the Euclidean norm between $H_{ij,LS}$ and $H_{ij,LS}^{IDFT}$.
The pseudo inverse of the matrix F' which is noted $F^{'\dagger} \in C^{CP \times M}$, provides a solution to equation 17. It can be used to transform the LS estimates in the time domain as proposed by equation 18 instead of $F^{'H}$ as previously proposed in equation 16. The use of the pseudo inverse allows the minimization of the power loss in the time domain which was at the origin of the "border effect".

$$h_{ij,LS}^{pseudoinverse} = F^{'\dagger} H_{ij,LS} \tag{18}$$

The pseudo inverse which is sometimes named *generalized inverse* was described by Moore in 1920 in *linear algebra* (Moore, 1920). This technique is often used for the resolution of linear equations system due to its capacity to minimize the *Euclidean norm* and then to tend towards the exact solution. The pseudo inverse $F^{'\dagger}$ of $F^{'}$ is defined as unique matrix satisfying all four following criteria (Penrose, 1955).

$$\begin{cases} 1 : F^{'} F^{'\dagger} F^{'} = F^{'} \\ 2 : F^{'\dagger} F^{'} F^{'\dagger} = F^{'\dagger} \\ 3 : (F^{'} F^{'\dagger})^H = F^{'} F^{'\dagger} \\ 4 : (F^{'\dagger} F^{'})^H = F^{\dagger'} F^{'} \end{cases} \tag{19}$$

4.1 Pseudo inverse computation using SVD

The pseudo inverse can be computed simply and accurately by using the singular value decomposition (Moore, 1920). Applying SVD to the matrix $F^{'}$ consists in decomposing $F^{'}$ in the following form:

$$F^{'} = USV^{H} \tag{20}$$

where $U \in C^{M \times M}$ and $V \in C^{CP \times CP}$ are unitary matrices and $S \in C^{M \times CP}$ is a diagonal matrix with non-negative real numbers on the diagonal, called singular values.
The pseudo inverse of the matrix $F^{'}$ with singular value decomposition is:

$$F^{'\dagger} = VS^{\dagger}U^{H} \tag{21}$$

It is important to note that $S^{\dagger}$ is formed by replacing every singular value by its inverse.

4.2 Impact of pseudo inverse conditional number on channel estimation accuracy

The accuracy of the estimated channel response depends on the calculation of the pseudo inverse $F^{'\dagger}$. The conditional number (CN) can give an indication of the accuracy of this operation (Yimin et al., 1991). The higher the CN is, the more the estimated channel response is degraded.

4.2.1 Definition of the conditional number

It is defined as the ratio between the greatest and the smallest singular values of the transfer matrix $F^{'}$. By noting $s \in C^{CP \times 1}$ the vector which contains the elements (the singular values) on the diagonal of the matrix S, CN is expressed as follows:

$$CN = \frac{max(s)}{min(s)} \tag{22}$$

where $max(s)$ and $min(s)$ give the greatest and the smallest singular values respectively.

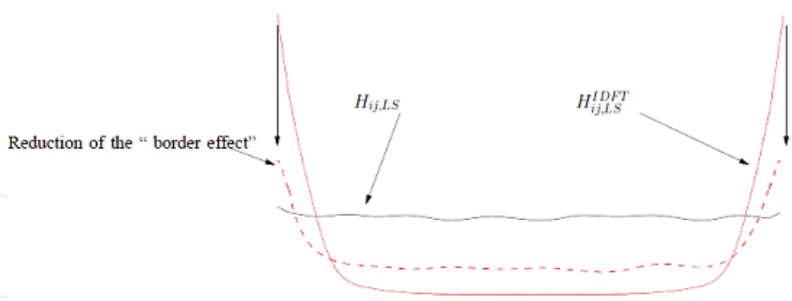

Fig. 4. Illustration of the "border effect" reduction

4.2.2 Behavior of the conditional number

It only evolves according to the number of modulated subcarriers. Fig.5 shows this behavior for different values of M when $N = 1024$ and $CP = 72$. When all the subcarriers are modulated (i.e when $M = N$), the CN is equal to 1. However when null carriers are inserted at the edge of the spectrum ($M < N$), the CN increases according to the number of non-modulated subcarriers ($N - N$) and can become very high.
We can note that if $M = 600$ as in 3GPP standard (where $N = 1024$, $CP = 72$ and $M = 600$), the CN is equal to $2.17\,10^{15}$.

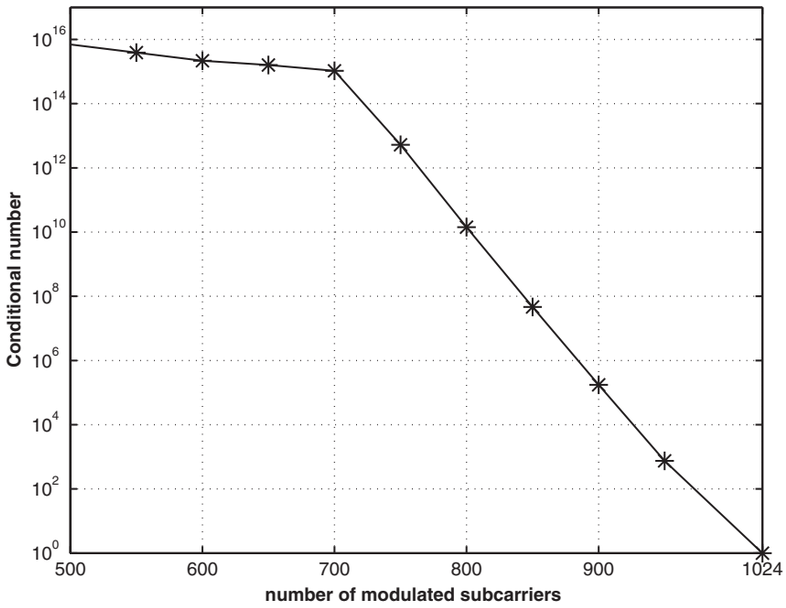

Fig. 5. Conditional number of $F^{'}$ versus the number of modulated subcarriers (M) where $CP = 72$ and $N = 1024$.

4.3 MSE performance of DFT with pseudo inverse channel estimation

System parameters for MSE performance evaluation are identical to those in section 3.3.

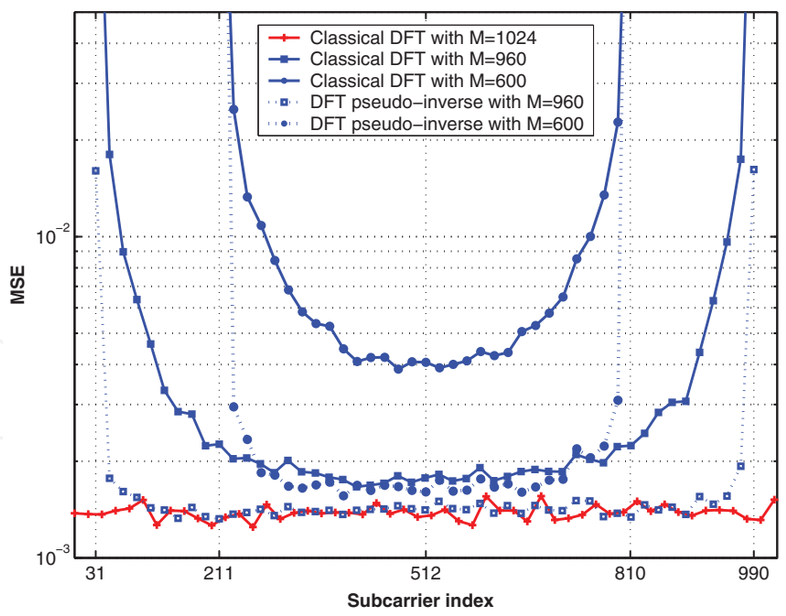

Fig. 6. Average mean square error versus subcarrier index for classical DFT and DFT pseudo inverse based channel estimation. The number of modulated subcarrier are $M = 960$ and $M = 600$. $N_t = 2$, $N_r = 2$, $N = 1024$ and $SNR = 10dB$

Fig.6 shows the MSE performance for different subcarriers when applying either classical DFT or DFT with pseudo inverse channel estimation methods. When null subcarriers are inserted

on the edges of the spectrum ($N \neq M$), the MSE performance of the classical DFT based channel estimation is degraded by the "border effect". As for CN, this "border effect" increases with the increasing number of null subcarriers. The DFT with pseudo inverse technique significantly reduces the "border effect" when the CN is low ($M = 960$ and $CN \simeq 100$). However, when the number of null subcarriers is large ($M = 600$) and the CN is largely increased ($CN = 2.17\ 10^{15}$), the MSE performance remains degraded.

5. DFT with truncated SVD channel estimation

The DFT with pseudo inverse technique previously described allows the reduction of the "border effect". But it remains insufficient when the number of null subcarriers is large. To further reduce this "border effect", it is necessary to attain a small CN in this operation. The aim of the proposed approach is to reduce both the "border effect" and the noise component by considering only the most significant singular values of matrix S.

5.1 Principle of DFT with truncated SVD channel estimation

To reduce the CN, the lowest singular values have to be eliminated. Hence, any singular value smaller than an optimized threshold (detailed in 5.2) is replaced by zero. The principle is depicted in Fig.7. The SVD calculation of matrix $F^{'}$ provides the matrices U, S and V (20). The matrix S becomes S_{T_h} where T_h is the number of considered singular values.

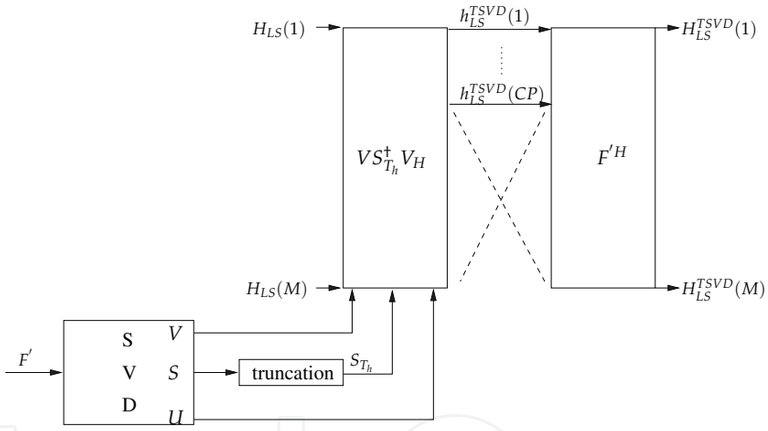

Fig. 7. Block diagram of DFT with Truncated SVD.

The channel impulse response after the smoothing process in the time domain can thus be expressed as follows:

$$h_{ij,LS}^{TSVD} = F_{T_h}^{'\dagger} H_{ij,LS} = VS_{T_h}^{\dagger} U^H H_{ij,LS} \tag{23}$$

$$h_{ij,LS,n}^{TSVD} = \begin{cases} F_{T_h}^{'\dagger} H_{ij,LS} = VS_{T_h}^{\dagger} U^H H_{ij,LS} & n < CP \\ 0 & otherwise \end{cases} \tag{24}$$

where $n = 0, ..., M-1$.
Finally $F^{'}$ of size $(CP \times M)$ is used to return to the frequency domain.

$$H^{ij,TSVD} = F^{'} h_{ij,LS}^{TSVD} \tag{25}$$

It is important to note the two following points:

- On the one hand, the "border effect" is obviously further reduced due to the reduction of the CN.
- On the other hand, the suppression of the lowest singular values allows the noise component in the estimated channel response to be reduced. The rank of the matrix $F^{'}$ is CP, which means that the useful power of the channel is distributed into CP virtual paths with singular values as weightings. The paths corresponding to the weakest singular values are predominated by noise and their elimination benefits the noise component reduction.

5.2 Threshold determination for DFT with truncated SVD

5.2.1 Discussion

The choice T_h ($\in 1, 2, ..., CP$) can be viewed as a compromise between the accuracy of the pseudo-inverse calculation and the CN magnitude. Its value will depend only on the system parameters: the number and position of the modulated subcarriers (M), the smoothing window size (CP) and the number of FFT points (N). All these parameters are predefined and are known prior to any channel estimation implementation. It is thus feasible to optimize the T_h value prior to any MIMO-OFDM system implementation.

To determine a good value of T_h, it is important to master its effect on the channel estimation quality i.e. on the matrix $F_{T_h}^{'\dagger}$ (24):

- When all the singular values of $F^{'}$ are considered, the CN of the matrix $F_{T_h}^{'\dagger}$ is very high and the accuracy of the estimated channel response is then degraded by the "border effect".
- However if insufficient singular values are used, the estimated channel response is also degraded due to a very large energy loss, even if the CN of $F_{T_h}^{'\dagger}$ is minimized.

The optimum value of T_h which provides a good compromise between these two phenomenons exists, as illustrated in the next subsection, for any MIMO-OFDM system.

5.2.2 Illustration

As previously seen, the adjustment of T_h enables the improvement of the channel estimation quality and its value depends only on the system parameters. To assess the value of T_h, we study here the behavior of the singular values of $F_{T_h}^{'\dagger}$ according to T_h. The same system parameters are considered: a 2×2 MIMO system, number of FFT points equal to 1024, $CP = 72$ and two different values of M (600 and 960). The orthogonality between the pilots from the different transmit antennas is again obtained by using null symbol insertion. The number of singular values of the matrix $F_{T_h}^{'\dagger}$ is then M/N_t.

Fig.8 illustrates the behavior of the $M/N_t = 300$ singular values of the matrix $F_{T_h}^{'\dagger}$ for different values of T_h when $M = 600$. For $T_h = 46, 45, 44$ the singular values of $F_{T_h}^{'\dagger}$ are the same on the first T_h indexes and almost null for the other ones. We can consider that the rank of the matrix $F_{T_h}^{'\dagger}$ becomes T_h instead of CP and that its CN is equal to 1. Therefore the "border effect" will surely be mitigated and the noise component be minimized. When $T_h \leq 43$, all the singular values become null due to a too large loss of energy.

The behavior of the singular values of $F_{T_h}^{'\dagger}$ can not be considered as constant for $T_h > 46$ and then the CN is high.

Differently, a moderated "border effect" is obtained when the number of non-modulated subcarriers is not too large ($M = 960$). Fig.9 illustrates the behavior of the singular values

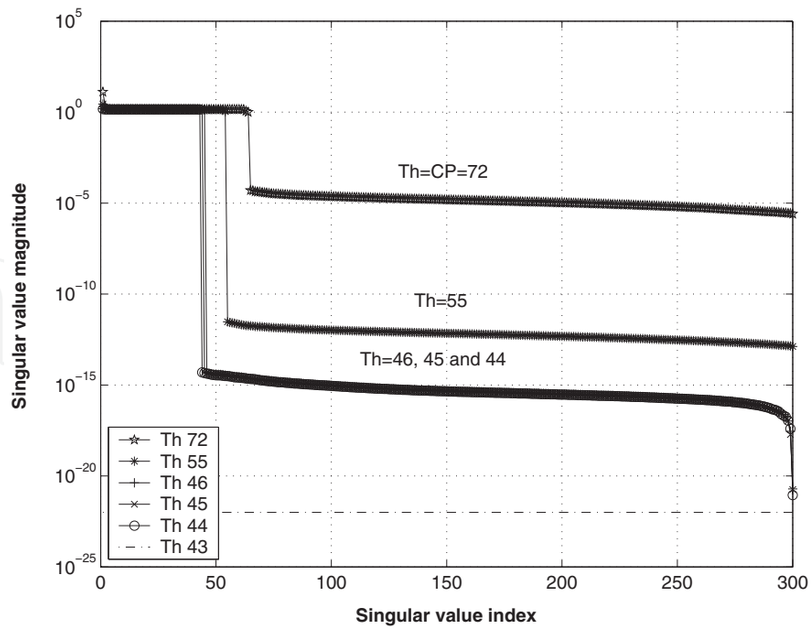

Fig. 8. Behavior of the $M/N_t = 300$ singular value of the matrix $F'^{\dagger}_{T_h}$ for $T_h = CP$, 55, 46, 45, 44 and 43. $N_t = 2$, $N_t = 2$, $CP = 72$, $N = 1024$ and $M = 600$.

of the matrix $F'^{\dagger}_{T_h}$ when $M = 960$. For $T_h = CP = 72$, the singular values of $F'^{\dagger}_{T_h}$ are the same on the first T_h indexes and almost zero for the other ones.

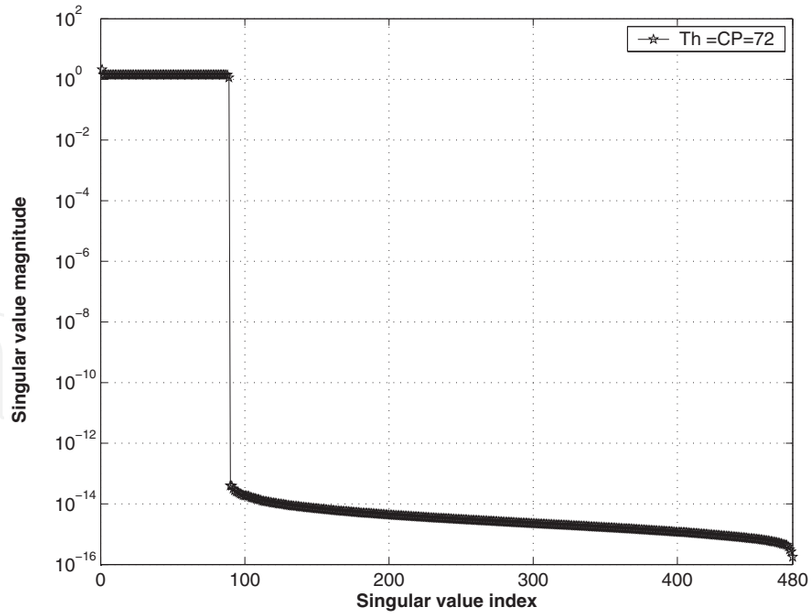

Fig. 9. Behavior of the $M/N_t = 480$ singular value of the matrix $F'^{\dagger}_{T_h}$ for $T_h = CP = 72$. $N_t = 2$, $N_t = 2$, $CP = 72$, $N = 1024$ and $M = 960$.

5.3 MSE performance of DFT with truncated SVD channel estimation

System parameters for MSE performance evaluation are identical to those in section 3.3.

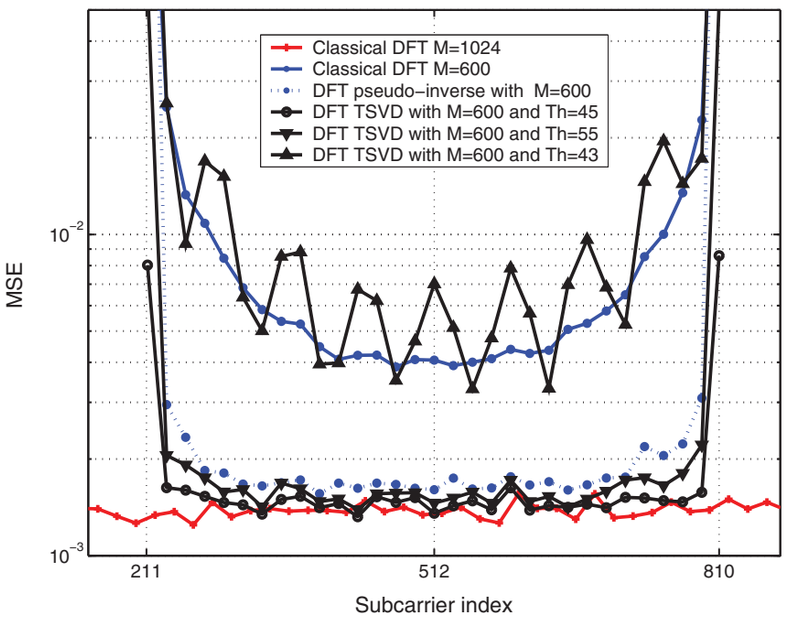

Fig. 10. Average mean square error versus subcarrier index for classical DFT, DFT pseudo inverse and DFT TSVD based channel estimation. The number of modulated subcarrier is $M = 600$. $N_t = 2$, $N_r = 2$, $N = 1024$ and $SNR = 10dB$

Fig.10 shows the MSE performance on the different subcarriers when applying either classical DFT, DFT with pseudo inverse channel or DFT with truncated SVD ($T_h = 43, 45, 55$) channel estimation methods. The DFT TSVD method with optimized T_h ($T_h = 45$) allows smaller MSE on all subcarriers to be obtained even at the edges of the spectrum. This is due to the minimization of the noise effect and the reduction of the CN provided by the TSVD calculation. Nevertheless this threshold has to be carefully assessed since a residual "border effect" is present when $T_h = 55$ and a large loss of channel power in the time domain brings poorer results when $T_h = 43$.

6. Applications

The performance of the three different DFT based channel estimation methods detailed in this paper are evaluated in the IEEE802.11n (typical *indoor*) and 3GPP/LTE (typical *outdoor*) system environments (downlink transmission).

6.1 Systems parameters

The simulation parameters are listed in Table 1 for both IEEE802.11n (802.11, 2007) and 3GPP/LTE (3GPP, 2008) configurations.

In IEEE802.11n, the channel (TGn channel models (Erceg et al., 2004)) can be assumed to be unchanged over the duration of 2 OFDM symbols due to quite slow variations. The orthogonality between training sequences on antennas 1 and 2 is obtained by using an orthogonal matrix. The estimated channel $H_{ij,LS}$ can be calculated for all the M modulated subcarriers due to the use of full pilot OFDM symbols.

Unlike in the IEEE802.11n system, in the 3GPP/LTE system, the time channel (SCME typical to urban macro channel model (Baum et al., 2005)) varies too much due to higher mobility. The orthogonality between training sequences in the 3GPP/LTE standard is thus based on the transmission on each subcarrier of pilot symbols on one antenna while null symbols are simultaneously sent on the other antennas. Therefore the LS channel estimates are calculated only for $\frac{M}{N_t} = 150$ subcarriers and interpolation is performed to obtain an estimation for all the modulated subcarriers.

system	802.11n	3GPP/LTE
Channel Model	TGn (Erceg et al., 2004)	SCME (Baum et al., 2005)
Sampling frequency (MHz)	20	15.36
Carrier frequency (GHz)	2.4	2
FFT size (N)	64	1024
OFDM symbol duration (μs)	4	71.35
Useful carrier (M)	52	600
Cyclic prefix (CP)	16	72
CP duration (μs)	0.80	4.69
MIMO scheme	SDM	double-Alamouti
MIMO rate (R_M)	1	1/2
$N_t \times N_r$	2×2	4×2
Modulation	QPSK	16QAM
Number of bit (m)	2	4
FEC	conv code (7,133,171)	turbo code (UMTS)
Coding Rate (R_c)	1/2	1/3

Table 1. Simulation Parameters

6.2 Simulation results

Perfect time and frequency synchronizations are assumed. Monte Carlo simulation results in terms of bit error rate (BER) versus $\frac{E_b}{N_0}$ are presented here for the different DFT based channel estimation methods: classical DFT, DFT with pseudo inverse and DFT with truncated SVD. The $\frac{E_b}{N_0}$ value can be inferred from the signal to noise ratio (SNR):

$$\frac{E_b}{N_0} = \frac{N_t}{mR_cR_M}.\frac{\sigma_s^2}{\sigma_n^2} = \frac{N_t}{mR_cR_M}.SNR \tag{26}$$

where σ_{noise}^2 and σ_x^2 represent the noise and signal variances respectively. R_c, R_M and m represent the coding rate, the MIMO scheme rate and the modulation order respectively.

Fig.11 and Fig.12 show the performance results in terms of BER versus $\frac{E_b}{N_0}$ for perfect, least square (LS), classical DFT, DFT with pseudo inverse ($DFT - T_h = CP$) and DFT with truncated SVD for (several T_h) channel estimation methods in 3GPP/LTE and 802.11n system environments respectively.

In the context of 3GPP/LTE, the classical DFT based method presents poorer results due to the large number of null carriers at the border of the spectrum (424 among 1024). The conditional number is as a consequence very high ($CN = 2.17\ 10^{15}$) and the impact of the "border effect" is very important. For this reason, the DFT with pseudo inverse ($DFT - T_h = CP =$

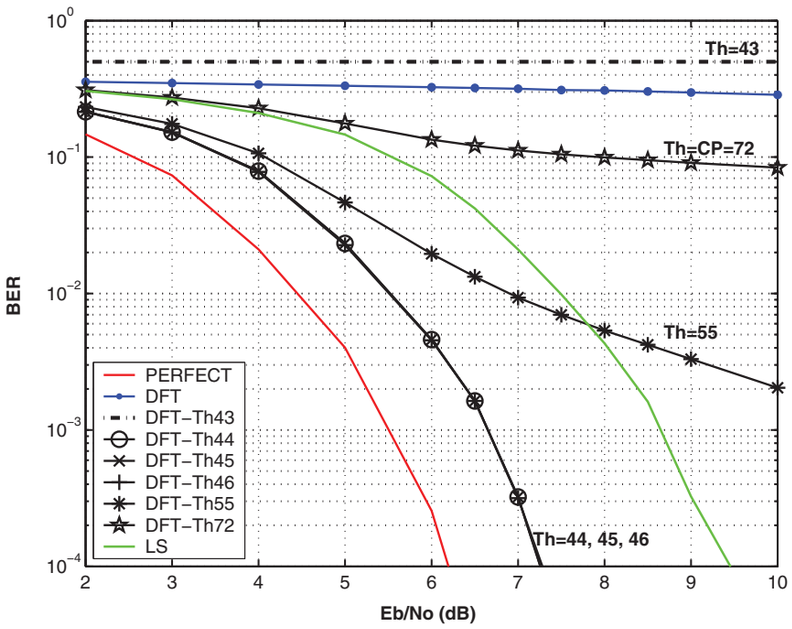

Fig. 11. BER versus $\frac{E_b}{N_0}$ for classical DFT, DFT pseudo inverse ($T_h = CP = 72$) and DFT with truncated SVD ($T_h = 55$, $T_h = 46$, $T_h = 45$, $T_h = 44$ and $T_h = 43$) based channel estimation methods in 3GPP context. $N_t = 4$, $N_r = 2$, $N = 1024$, $CP = 72$ and $M = 600$

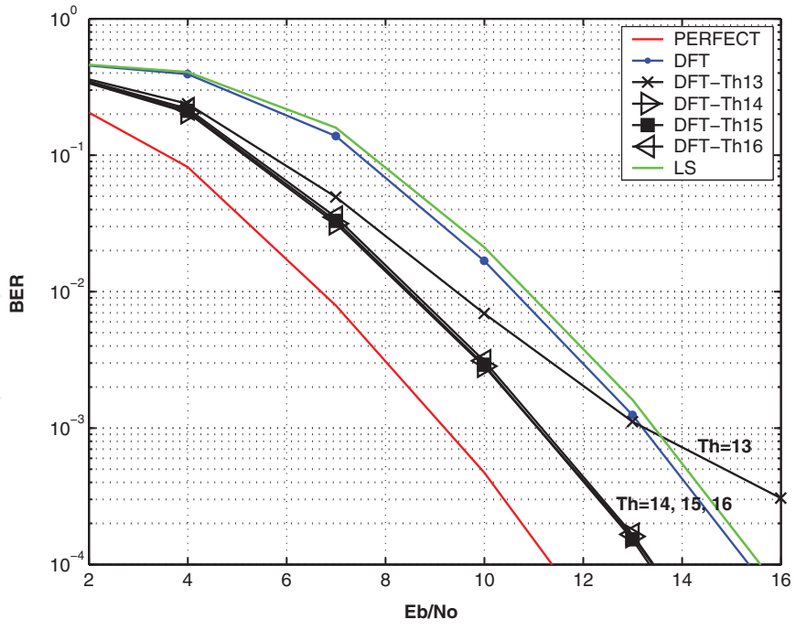

Fig. 12. BER versus $\frac{E_b}{N_0}$ for classical DFT, DFT pseudo inverse ($T_h = CP = 16$) and DFT with truncated SVD ($T_h = 15$, $T_h = 14$ and $T_h = 13$) based channel estimation methods in 802.11n context. $N_t = 2$, $N_r = 2$, $N = 1024$, $CP = 72$ and $M = 600$

72) can not greatly improve the accuracy of the estimated channel response. The classical DFT and the DFT with pseudo inverse estimated channel responses are thus considerably degraded compared to the *LS* one. The DFT with a truncated SVD technique and optimized T_h (T_h=46,45,44) greatly enhances the accuracy of the estimated channel response by both reducing the noise component and eliminating the impact of the "border effect" (up to 2dB gain compared to LS). This last method presents an error floor when $T_h = 55$ due to the fact that the "border effect" is still present and very bad results are obtained when T_h is small ($T_h = 43$) due to the large loss of energy.
Comparatively, in the context of 802.11n, the number of null carriers is less important and the classical DFT estimated channel response is not degraded even if it does not bring about any improvement compared to the LS. The pseudo inverse technique completely eliminates the "border effect" and thus its estimation ($DFT - T_h = CP = 16$) is already very reliable. DFT with a truncated SVD channel estimation method does not provide any further performance enhancement as the "border effect" is quite limited in this system configuration.

7. Conclusion

Several channel estimation methods have been investigated in this paper regarding the MIMO-OFDM system environment. All these techniques are based on DFT and are so processed through the time transform domain. The key system parameter, taken into account here, is the number of null carriers at the spectrum extremities which are used on the vast majority of multicarrier systems. Conditional number magnitude of the transform matrix has been shown as a relevant metric to gauge the degradation on the estimation of the channel response. The limit of the classical DFT and the DFT with pseudo inverse techniques has been demonstrated by increasing the number of null subcarriers which directly generates a high conditional number. The DFT with a truncated SVD technique has been finally proposed to completely eliminate the impact of the null subcarriers whatever their number. A technique which allows the determination of the truncation threshold for any MIMO-OFDM system is also proposed. The truncated SVD calculation is constant and depends only on the system parameters: the number and position of the modulated subcarriers, the cyclic prefix size and the number of FFT points. All these parameters are predefined and are known at the receiver side and it is thus possible to calculate the truncated SVD matrix in advance. Simulation results in 802.11n and 3GPP/LTE contexts have illustrated that DFT with a truncated SVD technique and optimized T_h is very efficient and can be employed for any MIMO-OFDM system.

8. References

Weinstein, S. B., and Ebert, P.M. (1971). Data transmission by frequency-division multiplexing using Discret Fourier Transform. *I*EEE Trans. Commun., Vol. 19, Oct. 1971, pp. 628-634.

Telatar, I. E.. (1995). Capacity of Multi-antenna Gaussien Channel. *A*TT Bell Labs tech. memo, Jun. 1995.

Alamouti, S. (1998). A simple transmit diversity technique for wireless communications, *I*EEE J. Select. Areas Communication, Vol. 16, Oct. 1998, pp. 1451-1458.

Tarokh, V., Japharkhani, H., and Calderbank, A. R.. (1999). Space-time block codes from orthogonal designs. *I*EEE Trans. Inform. Theory, Vol. 45, Jul. 1999, pp. 1456-1467.

Boubaker, N., Letaief, K.B., and Murch, R.D. (2001). A low complexity multi-carrier BLAST architecture for realizing high data rates over dispersive fading channels. Proceedings of VTC 2001 Spring, 10.1109/VETECS.2001.944489, Taipei, Taiwan, May 2001.

Winters, J. H. (1987). On the capacity of radio communication systems with diversity in a Rayleigh fading environment. *I*EEE J. Select. Areas Commun., Vol.5, June 1987, pp. 871-878.

Foschini, G. J (1996). Layered space-time architecture for wireless communication in a fading environment when using multi-element antennas. *B*ell Labs Tech. J., Vol. 5, 1996, pp. 41-59.

Zhao, Y., and Huang, A. (1997). A Novel Channel Estimation Method for OFDM Mobile Communication Systems Based on Pilot Signals and Transform-Domain. Proceedings of IEEE 47th VTC, 10.1109/VETEC.1997.605966, Vol. 47, pp. 2089-2093, May 1997.

Morelli, M., and Mengali., U. (2001). A comparison of pilot-aided channel estimation methods for OFDM systems. *I*EEE Transactions on Signal Processing, Vol. 49, Jan. 2001, pp. 3065-3073.

3GPP (2008), 3GPP TS 36.300 V8.4.0: E-UTRA and E-UTRAN overall description, Mar. 2008.

Doukopoulos, X.G., and Legouable, R. (2007). Robust Channel Estimation via FFT Interpolation for Multicarrier Systems. *P*roceedings of IEEE 65th VTC-Spring, 10.1109/VETECS.2007.386, pages 1861-1865, 2007.

Van de Beek, J., Edfors, O., Sandell, M., Wilson, S. K. and Borjesson, P.O. (1995). On Channel Estimation in OFDM Systems. *P*roceedings of IEEE VTC 1995, 10.1109/VETEC.1995.504981, pp. 815-819, Chicago, USA, Sept. 1995.

Auer, G. (2004). Channel Estimation for OFDM with Cyclic delay Diversity. *P*roceedings of PIMRC 2004, 15th IEEE International Symposium on IEEE, 10.1109/PIMRC.2004.1368308, Vol. 3, pp. 1792-1796.

*D*raft-P802.11n-D2.0. IEEE P802.11nTM, Feb. 2007.

Le Saux, B., Helard, M., and Legouable, R. (2007). Robust Time Domaine Channel Estimation for MIMO-OFDM Downlink System. *P*roceedings of MC-SS, Herrsching, Allemagne, Vol. 1, pp 357-366, May 2007.

Baum, D.S., Hansen, J., and Salo J. (2005). An interim channel model for beyond-3g systems: extending the 3gpp spatial channel model (smc). *P*roceedings of VTC, 10.1109/VETECS.2005.1543924, Vol. 5, pp 3132-3136, May 2005.

Moore, E. H. (1920). On the reciprocal of the general algebraic matrix. *B*ulletin of the American Mathematical Society, Vol. 26, pp 394-395, 1920.

Penrose, R. (1955). A generalized inverse for matrices. *P*roceedings of the Cambridge Philosophical Society 51, pp 406-413, 1955.

Yimin W. and al. (1991). Componentwise Condition Numbers for Generalized Matix Inversion and Linear least sqares. *A*MS subject classification, 1991.

Erceg V. and al. (2004). TGn channel models. IEEE 802.11-03/940r4, May 2004.

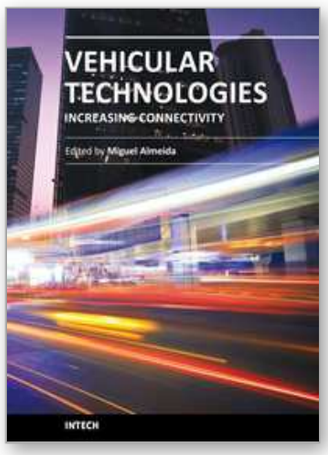

Vehicular Technologies: Increasing Connectivity
Edited by Dr Miguel Almeida

ISBN 978-953-307-223-4
Hard cover, 448 pages
Publisher InTech
Published online 11, April, 2011
Published in print edition April, 2011

This book provides an insight on both the challenges and the technological solutions of several approaches, which allow connecting vehicles between each other and with the network. It underlines the trends on networking capabilities and their issues, further focusing on the MAC and Physical layer challenges. Ranging from the advances on radio access technologies to intelligent mechanisms deployed to enhance cooperative communications, cognitive radio and multiple antenna systems have been given particular highlight.

How to reference
In order to correctly reference this scholarly work, feel free to copy and paste the following:

Moussa Diallo,Maryline Hélard, Laurent Cariou and Rodrigue Rabineau (2011). DFT Based Channel Estimation Methods for MIMO-OFDM Systems, Vehicular Technologies: Increasing Connectivity, Dr Miguel Almeida (Ed.), ISBN: 978-953-307-223-4, InTech, Available from: http://www.intechopen.com/books/vehicular-technologies-increasing-connectivity/dft-based-channel-estimation-methods-for-mimo-ofdm-systems

INTECH
open science | open minds

InTech Europe
University Campus STeP Ri
Slavka Krautzeka 83/A
51000 Rijeka, Croatia
Phone: +385 (51) 770 447
Fax: +385 (51) 686 166
www.intechopen.com

InTech China
Unit 405, Office Block, Hotel Equatorial Shanghai
No.65, Yan An Road (West), Shanghai, 200040, China
中国上海市延安西路65号上海国际贵都大饭店办公楼405单元
Phone: +86-21-62489820
Fax: +86-21-62489821

IntechOpen